JOURNAL OF ENZYME INHIBITION AND MEDICINAL CHEMISTRY
2019, VOL. 34, NO. 1, 110–116
https://doi.org/10.1080/14756366.2018.1530994

Taylor & Francis
Taylor & Francis Group

RESEARCH PAPER

OPEN ACCESS Check for updates

# Synthesis and cytotoxic activities of novel copper and silver complexes of 1,3-diaryltriazene-substituted sulfonamides

Dilek Canakci[a], Ismail Koyuncu[b], Nabih Lolak[c], Mustafa Durgun[d], Suleyman Akocak[c] and Claudiu T. Supuran[e]

[a]Department of Chemistry, Vocational School of Technical Sciences, Adiyaman University, Adiyaman, Turkey; [b]Faculty of Medicine, Department of Biochemistry, Harran University, Sanliurfa, Turkey; [c]Faculty of Pharmacy, Department of Pharmaceutical Chemistry, Adiyaman University, Adiyaman, Turkey; [d]Faculty of Arts and Sciences, Deparment of Chemistry, Harran University, Sanliurfa, Turkey; [e]NEUROFARBA Department, Sezione di Scienze Farmaceutiche, Università degli Studi di Firenze, Florence, Italy

**ABSTRACT**

In this study, a series of 10 novel copper (II) and silver complexes of 1,3-diaryltriazene-substituted sulfonamides was synthesised. All the synthesised ligands and their metal complexes were assessed for *in vitro* cytotoxicity against human colorectal adenocarcinoma (DLD-1), cervix carcinoma (HeLa), breast adenocarcinoma (MDA-MB-231), colon adenocarcinoma (HT-29), endometrial adenocarcinoma (ECC-1), prostate cancer (DU-145 and PC-3), normal embryonic kidney (HEK-293), normal prostate epithelium (PNT-1A), and normal retinal pigment epithelium (ARPE-19) cells. Most of the metal complexes from the series showed to be more active against all cancerous cells than the uncomplexed 1,3-diaryltriazene-substituted sulfonamides, and lower cytotoxic effects observed on normal cells. Most of the Cu (II) and Ag (I) metal complexes from the presented series showed high cytotoxic activity against HeLa cells with $IC_{50}$ values ranging from 2.08 to >300 μM. Specifically, compound $L_3$-Ag showed one of the highest cytotoxicity against all cancer cell lines with $IC_{50}$ values between 3.30 to 16.18 μM among other tested compounds.

**ARTICLE HISTORY**
Received 4 September 2018
Revised 26 September 2018
Accepted 28 September 2018

**KEYWORDS**
Metal complexes; triazene; cancer cells; sulfonamides; cytotoxicity

## 1. Introduction

Cancer is a group of the most fatal forms of diseases characterised by abnormal and uncontrolled cell proliferation. Cancer is the second most public cause of death after cardiovascular diseases across the world for men and women. On the other hand, incidence ratio is expected to increase dramatically in the near future. The high incidence and mortality ratio of cancer are due to the fact that there are more than 200 types of cancer and it is very hard to discover most of them in the early stage. For all these reasons, most majority of current research focused on cancer treatment with biologically more potent and less toxic way by using specific methods and techniques[1–3].

Primary sulfonamides and their isoesters (sulfamides, sulfamates) constitute an important class of drugs with a wide variety of pharmacological applications[4–6]. Sulfonamides were also having an important place in drug discovery studies and continue to be the one of the most investigated compounds possessing different pharmacological activities such as, antibacterial, diuretic, anticarbonic anhydrase, protease inhibitory activity and more recently antitumor, among others[4–8]. Recently, one of the sulfonamide based CA inhibitor compound, which is ureido-substituted SLC-0111 was shown to be a highly effective hCA IX/XII inhibitor and reached to Phase I/II clinical trials for the treatment of advanced, metastatic breast cancer[9–11].

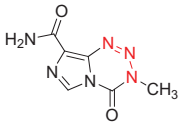
Temozolamide (TMZ)

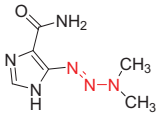
Dacarbazine (DTIC)

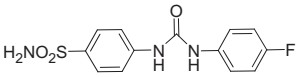
SLC-0111

Triazenes (−N = N − NH−) are a diverse group of compounds which have been broadly investigated for synthetic reaction transformations and used for different applications such as natural product synthesis, combinatorial chemistry, and biomedical applications, among others[12,13]. The 1,3-diaryltriazene scaffold is one of the most interesting core owing to broad biological activities such as antibacteriel, antifungal, efficient carbonic anhydrase inhibitors, and their abundant use is in the development of novel anticancer molecules[12,13]. On the other hand, triazene compounds of clinical interest (such as Temozolamide and Dacarbazine), are a group of alkylating agents with excellent pharmacokinetic properties and limited toxicity[12,13].

Triazene moieties can serve as monodentate binding through a terminal or central nitrogen, bidentate (N1, N3)-chelating to form bidentate complexes, and bridging ligands through (N1, N3)-bridging between two metal centers to from metallocycles over a wide variety of transition metal complexes[14,15]. Since metal-based drugs gained much attention after the discovery of cisplatin as an

CONTACT Ismail Koyuncu ismailkoyuncu@gmail.com Faculty of Medicine, Department of Biochemistry, Harran University, Sanliurfa, Turkey; Suleyman Akocak akocaksuleyman@gmail.com Faculty of Pharmacy, Department of Pharmaceutical Chemistry, Adiyaman University, 02040 Adiyaman, Turkey; Claudiu T. Supuran claudiu.supuran@unifi.it Università degli Studi di Firenze, NEUROFARBA Department, Sezione di Scienze Farmaceutiche, Via Ugo Schiff 6, 50019 Sesto Fiorentino, Florence, Italy

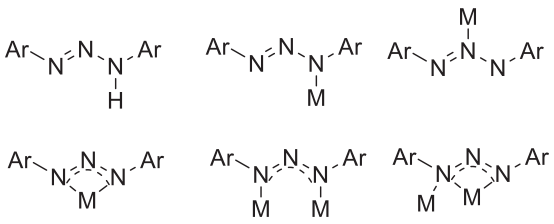

Scheme 1. General binding modes of triazene ligands.

antitumor agent, 1,3-diaryltriazene based metal complexes started to be investigated more as a metallo-pharmaceuticals for several diseases especially for cancer (Scheme 1)[14,15].

Generally, metals are essential components of cells chosen by nature[16]. They are frequently found in the enzyme catalytic domain[17] and are involved in multiple biological processes, from the exchange of electrons to catalysis and structural roles[17]. They are extensively used in cellular activities. Such metals include gallium, zinc, cobalt, silver, vanadium, strontium, manganese and copper, which are required in trace amounts to trigger catalytic processes[18]. To this end, a balance between cellular need and the amount available in the body is important for the normal physiological state. Recently, there has been a growing demand for metal complex compounds in the treatment of cancer because of their improved biological activity than their corresponding free ligands[19].

It has been well accepted that hybrid molecules through the combination of different scaffolds and pharmacophores into a single compound may lead to the improved cytotoxic potency of compounds with synergistic effect. According to literature knowledge and our previous studies[13–15,20], in the current work, novel copper (II) and silver complexes incorporating 1,3-diaryltriazene-substituted sulfonamides were synthesised in attempt to obtain possible active compounds having cytotoxic activities against DLD-1, HeLa, MDA-MB-231, HT-29, ECC-1, DU-145, PC-3, HEK-293, PNT-1A, and ARPE-19 cancer cell lines. Our aim was to investigate new metal complexes to have a potent cytotoxic effect with a low toxicity.

## 2. Materials and methods

### 2.1. General

All chemicals and anhydrous solvents were purchased from Sigma-Aldrich, Merck, Alfa Aesar and TCI and used without further purification. Melting points (mp) were determined with SMP30 melting point apparatus in open capillaries and are uncorrected. FT-IR spectra were recorded by using Perkin Elmer Spectrum 100 FT-IR spectrometer. Ultraviolet–visible (UV–vis) absorption spectra were recorded on Shimadzu UV-2101 spectrophotometer in DMSO. Nuclear Magnetic Resonance ($^1$H-NMR and 13C-NMR) spectra of compounds were recorded using a Bruker Advance III 300 MHz spectrometer in DMSO-$d_6$ and TMS as an internal standard operating at 300 MHz for $^1$H-NMR and 75 MHz for $^{13}$C-NMR. Thin layer chromatography (TLC) was carried out on Merck silica gel 60 $F_{254}$ plates.

The ligands 3–(3-(4-fluorophenyl)triaz-1-en-1-yl) benzenesulfonamide (**$L_1$**), 3–(3-(4-methoxyphenyl)triaz-1-en-1-yl) (**$L_2$**), benzenesulfonamide 4–(3–(3-sulfamoylphenyl)triaz-2-en-1-yl) benzoic acid (**$L_3$**), 3–(3-(3,4-dimethoxyphenyl)triaz-1-en-1-yl) benzenesulfonamide (**$L_4$**), and 3-(3-(3,5-dimethylphenyl)triaz-1-en-1-yl)benzenesulfonamide (**$L_5$**) were synthesised and characterised as previously described by us[20].

### 2.2. General procedure for the preparation of coordination compounds ($L_{1-5}$ Cu)

The copper complexes of 1,3-diaryltriazene-substituted metanilamides were prepared using chemical precipitation of ion $Cu^{2+}$ with a molar ratio of 1:1. Briefly, Copper(II) acetate monohydrate (1.0 mmol) was dissolved in ethanol (10 ml) at room temperature. The ligands (**$L_{1-5}$**) (1.0 mmol) dissolved in ethanol (10 ml) were added into resulting solution drop by drop. The mixture was refluxed for 3 h and after cooling, the resulting solution was partially evaporated. The precipitate was separated by filtration, washed with 1:1 (v/v ethanol/water) and the pure complexes were dried in a desiccator over anhydrous calcium chloride at room temperature.

#### 2.2.1. $L_1$-Cu

Yield: 41%; Color: brown solid; mp: >300 $^0$C; UV–Vis (DMSO, nm): 232, 261, 305, 359, 460; FT-IR ($cm^{-1}$): 3374, 3077 ($NH_2$), 1666 (C=C), 1437 (N=N), 1330 (asymmetric), 1162 (symmetric) (S=O); $^1$H-NMR (DMSO-$d_6$, 300 MHz, δ ppm): 7. 92 (s, 1H, Ar-H), 7.70–7.42 (m, 5H, Ar-H), 7.49 (s, 2H, $-SO_2NH_2$), 7.32 (t, 2H, $J = 3.3$, Ar-H): 13C-NMR (DMSO-$d_6$, 75 MHz, δ ppm): 158.6, 151.9, 145.6, 138.2, 130.4, 124.8, 123.5, 119.8, 116.6, 115.7;

#### 2.2.2. $L_2$-Cu

Yield: 45%; Color: brown solid; mp: >300 $^0$C; UV–Vis (DMSO, nm): 239, 254, 303, 409, 461; FT-IR ($cm^{-1}$): 3256, 3000 ($NH_2$), 1586 (C=C), 1457 (N=N), 1320 (asymmetric), 1155 (symmetric) (S=O); $^1$H-NMR (DMSO-$d_6$, 300 MHz, δ ppm): 7. 95 (s, 1H, Ar-H), 7.85–7.78 (m, 5H, Ar-H), 7.75–7.68 (m, 2H, Ar-H), 7.54 (s, 2H, $-SO_2NH_2$), 3.86 (s, 3H, $-OCH_3$): 13C-NMR (DMSO-$d_6$, 75 MHz, δ ppm): 159.4, 151.2, 145.9, 138.4, 130.2, 124.5, 123.7, 119.9, 116.4, 115.3, 55.6;

#### 2.2.3. $L_3$-Cu

Yield: 38%; Color: brown solid; mp: >300 $^0$C; UV–Vis (DMSO, nm): 245, 255, 278, 364, 440; FT-IR ($cm^{-1}$): 3570, 3075 ($NH_2$), 1591 (C=C), 1471, 1330 (asymmetric), 1124 (symmetric) (S=O); $^1$H-NMR (DMSO-$d_6$, 300 MHz, δ ppm): 12.92 (br.s, 1H, $-COOH$), 7. 90 (s, 1H, Ar-H), 7.75–7.58 (m, 5H, Ar-H), 7.50 (s, 2H, $-SO_2NH_2$), 7.45–7.33 (m, 2H, Ar-H): 13C-NMR (DMSO-$d_6$, 75 MHz, δ ppm): 179.5, 159.1, 151.7, 145.9, 138.8, 130.7, 124.2, 123.5, 119.7, 116.8, 115.6;

#### 2.2.4. $L_4$-Cu

Yield: 43%; Color: brown solid; mp: >300 $^0$C; UV–Vis (DMSO, nm): 233, 246, 260, 309, 363, 453; FT-IR ($cm^{-1}$): 3412, 2956 ($NH_2$), 1627 (C=C), 1415 (N=N), 1350 (asymmetric), 1110 (symmetric) (S=O); $^1$H-NMR (DMSO-$d_6$, 300 MHz, δ ppm): 8.25 (s, 1H, Ar-H), 8.15–8.09 (m, 1H, Ar-H), 7.73–7.61 (m, 3H, Ar-H), 7.49 (s, 2H, $-SO_2NH_2$), 7.39 (s, 1H, Ar-H), 6.45 (s, 1H, Ar-H), 3.85 (s, 3H, $-OCH_3$), 3.80 (s, 3H, $-OCH_3$),: 13C-NMR (DMSO-$d_6$, 75 MHz, δ ppm): 160.5, 151.9, 146.3, 139.7, 138.5, 131.2, 130.6, 125.7, 123.6, 119.1, 116.6, 115.3, 55.9, 55.5;

#### 2.2.5. $L_5$-Cu

Yield: 37%; Color: brown solid; mp: >300 °C; UV–Vis (DMSO, nm): 226, 279, 310, 361, 524; FT-IR ($cm^{-1}$): 3341, 3080 ($NH_2$), 1598 (C=C), 1484 (N=N), 1310 (asymmetric), 1124 (symmetric) (S=O); $^1$H-NMR (DMSO-$d_6$, 300 MHz, δ ppm): 8.10 (s, 1H, Ar-H), 7.92–7.68 (m, 2H, Ar-H), 7.70–7.64 (m, 2H, Ar-H), 7.50 (s, 2H, $-SO_2NH_2$), 6.48

(s, 2H, Ar-H), 2.52 (s, 6H, $-CH_3$): 13C-NMR (DMSO-$d_6$, 75 MHz, δ ppm): 160.1, 151.5, 146.8, 139.2, 131.1, 125.7, 123.4, 119.5, 116.1, 115.3, 21.5;

### 2.3. General procedure for the preparation of coordination compounds ($L_{1-5}$ Ag)

Ethanol (20 ml) and silver acetate (1 mmol) were taken into boiling flask and stirred for 30 min at room temperature. At the end of the period, $\mathbf{L_{1-5}}$ (1 mmol) dissolved in ethanol (10 ml) was added drop by drop into solution. The mixture was thoroughly mixed and allowed to reflux for 3 h. The resulting solution was partially evaporated. The precipitate was separated by filtration, washed with 1:1 (v/v ethanol/water) and the pure complexes were dried in a desiccator over anhydrous calcium chloride at room temperature.

#### 2.3.1. $L_1$-Ag

Yield: 36%; Color: light brown solid; mp: >300 °C; UV–Vis (DMSO, nm): 259, 288, 413, 454; FT-IR ($cm^{-1}$): 3420, 3069 ($NH_2$), 1596 (C=C), 1430 (N=N), 1332 (asymmetric), 1157 (symmetric) (S=O); $^1$H-NMR (DMSO-$d_6$, 300 MHz, δ ppm): 7. 90 (s, 1H, Ar-H), 7.72–7.43 (m, 5H, Ar-H), 7.48 (s, 2H, $-SO_2NH_2$), 7.30 (t, 2H, $J = 3.3$, Ar-H): $^{13}$C-NMR (DMSO-$d_6$, 75 MHz, δ ppm): 158.9, 151.3, 145.7, 138.1, 130.3, 124.3, 123.8, 119.1, 116.7, 115.4;

#### 2.3.2. $L_2$-Ag

Yield: 25%; Color: light brown solid; mp: >300 °C; UV–Vis (DMSO, nm): 247, 294; FT-IR ($cm^{-1}$): 3234, 3000 ($NH_2$), 1580 (C=C), 1431 (N=N), 1325 (asymmetric), 1153 (symmetric) (S=O); $^1$H-NMR (DMSO-$d_6$, 300 MHz, δ ppm): 7. 93 (s, 1H, Ar-H), 7.84–7.75 (m, 5H, Ar-H), 7.74–7.66 (m, 2H, Ar-H), 7.51 (s, 2H, $-SO_2NH_2$), 3.85 (s, 3H, $-OCH_3$): $^{13}$C-NMR (DMSO-$d_6$, 75 MHz, δ ppm): 159.9, 151.4, 145.5, 138.2, 130.6, 124.7, 123.2, 119.5, 116.3, 115.1, 55.5;

#### 2.3.3. $L_3$-Ag

Yield: 36%; Color: light brown solid; mp: >300 °C; UV–Vis (DMSO, nm): 268, 276, 312, 359, 423; FT-IR ($cm^{-1}$): 3229, 3065 ($NH_2$), 1690 (C=O), 1602 (C=C), 1427 (N=N), 1334 (asymmetric), 1159 (symmetric) (S=O); $^1$H-NMR (DMSO-$d_6$, 300 MHz, δ ppm): 12.90 (br.s, 1H, −COOH), 7. 88 (s, 1H, Ar-H), 7.73–7.59 (m, 5H, Ar-H), 7.49 (s, 2H, $-SO_2NH_2$), 7.43–7.34 (m, 2H, Ar-H): $^{13}$C-NMR (DMSO-$d_6$, 75 MHz, δ ppm): 179.2, 159.4, 151.5, 145.6, 138.2, 130.5, 124.6, 123.4, 119.5, 116.9, 115.3;

#### 2.3.4. $L_4$-Ag

Yield: 36%; Color: light brown solid; mp: >300 °C; UV–Vis (DMSO, nm): 259, 288, 413, 454; FT-IR ($cm^{-1}$): 3420, 3069 ($NH_2$), 1596 (C=C), 1430 (N=N), 1345 (asymmetric), 1157 (symmetric) (S=O); $^1$H-NMR (DMSO-$d_6$, 300 MHz, δ ppm): 8.22 (s, 1H, Ar-H), 8.11–8.05 (m, 1H, Ar-H), 7.70–7.60 (m, 3H, Ar-H), 7.48 (s, 2H, $-SO_2NH_2$), 7.37 (s, 1H, Ar-H), 6.44 (s, 1H, Ar-H), 3.83 (s, 3H, $-OCH_3$), 3.79 (s, 3H, $-OCH_3$),: $^{13}$C-NMR (DMSO-$d_6$, 75 MHz, δ ppm): 160.3, 151.7, 146.5, 139.5, 138.1, 131.6, 130.7, 125.3, 123.2, 119.4, 116.1, 115.4, 55.8, 55.4;

#### 2.3.5. $L_5$-Ag

Yield: 32%; Color: light brown solid; mp: >300 °C; UV–Vis (DMSO, nm): 231, 250, 293, 531; FT-IR ($cm^{-1}$): 3368, 3255 ($NH_2$), 1589 (C=C), 1434 (N=N), 1320 (asymmetric), 1163 (symmetric) (S=O); $^1$H-NMR (DMSO-$d_6$, 300 MHz, δ ppm): 8.09 (s, 1H, Ar-H), 7.90–7.69 (m, 2H, Ar-H), 7.65–7.60 (m, 2H, Ar-H), 7.48 (s, 2H, $-SO_2NH_2$), 6.45 (s, 2H, Ar-H), 2.50 (s, 6H, $-CH_3$): $^{13}$C-NMR (DMSO-$d_6$, 75 MHz, δ ppm): 160.0, 151.4, 146.5, 139.1, 131.0, 125.4, 123.2, 119.2, 116.5, 115.8, 21.6;

### 2.4. In vitro cytotoxic activity

#### 2.4.1. Cell cultures

The cells studied were obtained from the American Type Culture Collection (ATCC, Manassas, VA), and included human colorectal adenocarcinoma (DLD-1), cervix carcinoma (HeLa), breast adenocarcinoma (MDA-MB-231), colon adenocarcinoma (HT-29), endometrial adenocarcinoma (ECC-1), prostate cancer (DU-145 and PC-3), normal embryonic kidney (HEK-293), normal prostate epithelium (PNT-1A), and normal retinal pigment epithelium (ARPE-19) cells. As recommended by ATCC, cells were subjected to propagation using DMEM-F12 and RPMI-1640 media, with supplements 10% fetal bovine serum, L-glutamine (2 mM), penicillin (100 U/mL) and streptomycin (100 mg/mL) in a humidified atmosphere (5% $CO_2$) at 37 °C. When the cultures reached 70–80% confluence, the cells were harvested using 0.25% trypsin (Sigma).

#### 2.4.2. Cytotoxicity assays and determination of $IC_{50}$

Cytotoxic activities were based on the reduction of (3–(4,5-dimethylthiazol-2-yl)-2,5-diphenyltetrazolium bromide) (MTT) by mitochondrial dehydrogenase of viable cells to give a blue formazan product which can be measured spectrophotometrically by UV–Vis measurements. MTT colorimetric assays were performed using 96 well plates. The cells were seeded in a 96 well plate at concentration $5.0 \times 10^4$ cells/well and incubated at 37 °C for 24 h. After treatment with various concentrations of the test compound (1, 5, 10, 25, 50, 100 and 200 μM), the cells were incubated for an additional 48 h at 37 °C. After incubation, the medium was removed, and the cells in each well were incubated with 100 μL MTT solution (5 mg/mL) for 4 h at 37 °C. MTT solutions were then discarded, and 100 μL DMSO were added to dissolve insoluble formazan crystals. Optical densities were measured at 570 nm (Varioskan Flash Multimode Reader, Thermo, Waltham, MA). Data were obtained from triplicate wells. Cytotoxic effects were determined in reference to negative controls (vehicle treated cells). Cytotoxicity was expressed as the mean percentage increase relative to the unexposed control (mean ± SD). All statistical analyses were performed using SPSS package program for Windows (Version 20, Chicago, IL). Control values were set to 0% cytotoxicity. Cytotoxicity data, where appropriate, were fitted to sigmoidal curves and a four-parameter logistic model was used to calculate the $IC_{50}$ values, the concentration of material causing 50% inhibition, compared to the untreated controls. 5-Fluorouracil (5-FU) was also used as a control agent[21,22].

## 3. Results and discussion

### 3.1. Synthesis and characterisation of the metal complexes

The copper (II) and silver complexes were synthesised from the reaction of the appropriate 1,3-diaryltriazene-substituted sulfonamide ligands and metal salt. The structures of Cu and Ag 1,3-diaryltriazene metal complexes ($Cu^{+2}$ and $Ag^{+}$) were elucidated by $^1$H-NMR, $^{13}$C-NMR, UV–Vis and FT-IR spectroscopic analysis.

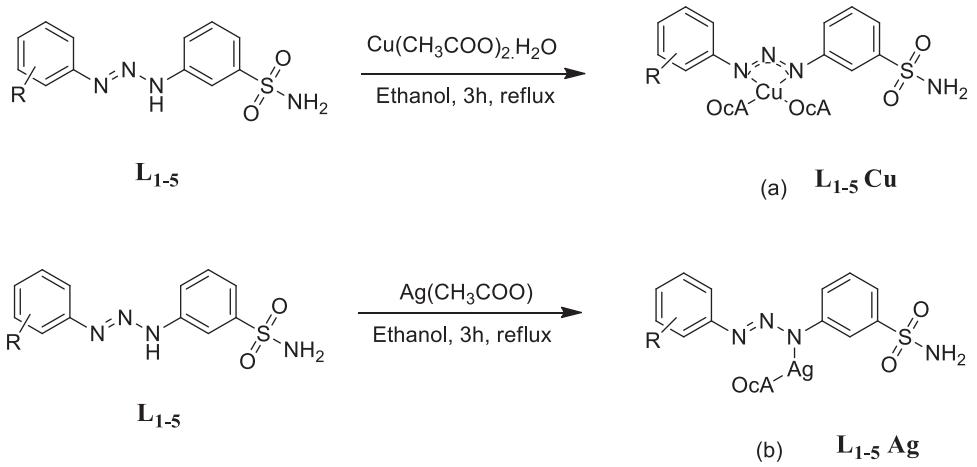


**R**= ($L_1$= 4-F, $L_2$= 4-MeO, $L_3$= 4-COOH, $L_4$= 3,4-diMeO, $L_5$= 3,5-diMe)

**Scheme 2.** General synthetic route of the novel copper (a) and silver (b) complexes.

**Table 1.** The UV–Vis spectra data of 1,3-diaryltriazene ligands and metal complexes.

| Compounds | A $\lambda_{max}$ | $\varepsilon_{max} \times 10^{-5}$ | B $\lambda_{max}$ | $\varepsilon_{max} \times 10^{-5}$ | C $\lambda_{max}$ | $\varepsilon_{max} \times 10^{-5}$ | D $\lambda_{max}$ | $\varepsilon_{max} \times 10^{-5}$ | $E_{CT}$ |
|---|---|---|---|---|---|---|---|---|---|
| $L_1$ | 233 | 0.389 | 309 | 3.289 | 360 | 3.148 | 401 | 2.637 | 3.133 |
| $L_2$ | 260 | 3.585 | 289 | 3.937 | 366 | 2.652 | 420 | 2.792 | 2.961 |
| $L_3$ | 254 | 1.629 | 303 | 3.547 | 360 | 3.323 | 416 | 2.949 | 2.990 |
| $L_4$ | 254 | 1.561 | 273 | 0.486 | 341 | 1.500 | 496 | 1.442 | 2.507 |
| $L_5$ | 255 | 2.881 | 294 | 3.730 | 341 | 1.503 | 497 | 3.374 | 2.502 |
| $L_1$-Cu | 262 | 3.850 | 288 | 4.663 | 353 | 2.914 | 427 | 2.641 | 2.913 |
| $L_2$-Cu | 254 | 2.294 | 303 | 3.645 | 360 | 3.399 | 461 | 4.364 | 2.698 |
| $L_3$-Cu | 234 | 3.842 | 281 | 5.273 | 361 | 3.113 | 422 | 2.819 | 2.947 |
| $L_4$-Cu | 260 | 1.448 | 309 | 3.142 | 363 | 3.020 | 453 | 3.145 | 2.745 |
| $L_5$-Cu | 222 | 4.383 | 279 | 6.561 | 366 | 2.474 | 411 | 2.581 | 3.026 |
| $L_1$-Ag | 248 | 4.537 | 287 | 5.096 | – | – | 438 | 4.104 | 2.839 |
| $L_2$-Ag | 247 | 1.996 | 285 | 1.913 | – | – | 447 | 3.286 | 2.782 |
| $L_3$-Ag | 268 | 3.483 | 312 | 3.529 | 359 | 3.332 | 423 | 3.177 | 2.940 |
| $L_4$-Ag | 256 | 2.154 | 293 | 3.676 | – | – | 531 | 3.373 | 2.342 |
| $L_5$-Ag | 259 | 2.846 | 292 | 2.540 | 367 | 2.857 | 480 | 3.509 | 2.591 |

$\lambda_{max}$: the wavelength at the absorption maxima(nm); $\varepsilon_{max}$: molar absoptivity coefficient(L/mol cm); $E_{CT}$: charge transfer energy(eV).

All spectral data were in agreement with calculated values of proposed structures (Scheme 2).

FT-IR spectra of all synthesised 1,3-diaryltriazene-substituted sulfonamides and metal complexes were recorded in the range of 450–4000 $cm^{-1}$. The FT-IR spectrum of ligands shows bands around 3350 and 3000 $cm^{-1}$. These bands resulted from stretching vibrations of protons (N–H) in the structure of triazene and sulfonamide. The band forming around 1600 $cm^{-1}$, on the other hand, represents ν(N=N) stretching vibration. The ν(N=N) stretching vibration band formed in the region of ν(C=O) stretching band because of the tautomeric forms of the compound. Another reason was ν(N-H) plane and out-of- plane bending vibrations. The peaks in the range of 1100–1380 $cm^{-1}$ were attributes to symmetric and assymmetric the ν(S=O) stretching frequency. Aromatic C–H stretching vibration bands were observed in the range of 2916–3017 $cm^{-1}$. Bands in the range of 1400–1590 $cm^{-1}$ occurred as a result of aromatic ν(C=C) and ν(N=N) stretching vibrations.

According to spectra of complexes, the most significant difference with ligand spectrum was in the range of 2900–3600 $cm^{-1}$. ν(N-H) bands which were considerably sharp in triazene gained a broad appearance as a result of the formation of complex. The reason for this was that formation of complex took place through metal and nitrogen atoms. Bands seen at around 3350 and 3250 $cm^{-1}$ in the spectrum of metal complexes belonged to ν(N–H) stretching vibration. Bands forming at around 2900 and 3000 $cm^{-1}$ occurred as a result of aromatic ν(C–H) stretching vibration. In addition, intensity of bands and the number of bands decreased as a result of complex formation. Aromatic ν(C–H) vibration band was not observed in the spectrum because it overlapped with ν(N–H) stretching vibration bands. While ν(N=N) stretching vibration band formed around 1590 $cm^{-1}$, aromatic ν(C=C) and ν(N–N) stretching vibration bands occurred at around 1550 and 1450 $cm^{-1}$, respectively. Another feature supporting the formation of complex was that some peaks were not seen in spectra of finger print site. The bands due to the metal-ligand stretching modes are expected to be present in the low frequency region between 650 and 200 $cm^{-1}$.

The UV–Vis absorption spectra of all 1,3-diaryltriazenes and metal complexes with $Cu^{+2}$ and $Ag^{+}$ were measured in DMSO in a concentration of $10^{-5}$ mol $L^{-1}$ in the wavelength range of 200–700 nm. Table 1 shows electronic absorption spectra of triazene ligands and cooper and silver complexes. Although the main structure of all the triazene compounds is similar, different shifts are seen in the UV–Vis spectrum due to the fact that the groups bound to the benzene ring are different. All compounds showed almost identical absorption maxima in the ultraviolet region in the range of 200–260 nm, corresponding to π→π* transitions of benzenoid system of the compounds. The band observed in the range 273–312 nm is assigned to low energy π→π* electronic transition

**Table 2.** Cytotoxicity of ligands $L_{1\text{-}5}$, metal complexes of $L_{1\text{-}5}$ Cu, $L_{1\text{-}5}$ Ag and 5-fluorouracil (5-FU) on tumor cell lines and normal cell lines.

| | $IC_{50}$ (μM)[a,b] | | | | | | | | | |
|---|---|---|---|---|---|---|---|---|---|---|
| | Cancer cell | | | | | | | Normal cell | | |
| Compound | DLD-1 | HeLa | MDA-MB-231 | HT-29 | ECC-1 | DU-145 | PC-3 | HEK-293 | PNT-1A | ARPE-19 |
| $L_1$ | 139.8 ± 11.0 | 178.8 ± 16 | 104.1 ± 28.2 | 79.4 ± 15.4 | 239.4 ± 27.5 | 29.0 ± 2.9 | 168.2 ± 18.5 | 131.7 ± 16.4 | 194.9 ± 23.5 | 279.2 ± 33.8 |
| $L_2$ | 223.0 ± 8.3 | 768 ± 6.5 | 144.4 ± 2.4 | 265.2 ± 30 | >300 | 154.4 ± 25.6 | 170.6 ± 20.5 | 145.7 ± 13.4 | >300 | >300 |
| $L_3$ | >300 | >300 | >300 | >300 | 197.0 ± 23.5 | 186.5 ± 20.6 | >300 | >300 | >300 | >300 |
| $L_4$ | >300 | >300 | 155.1 ± 2.6 | >300 | >300 | 181.9 ± 23.4 | 299.4 ± 32.3 | >300 | 237.1 ± 26.8 | >300 |
| $L_5$ | 223.6 ± 12.4 | 65.1 ± 4.5 | 144.1 ± 18.6 | 111.6 ± 16.5 | 131.6 ± 13.1 | 97.8 ± 9.7 | 131.0 ± 12.4 | 102.7 ± 10.2 | 177.4 ± 20.5 | >300 |
| $L_1$-Cu | 47.1 ± 4.7 | 5.0 ± 0.4 | 116.8 ± 14.2 | 198.9 ± 24.3 | 26.2 ± 2.6 | 104.9 ± 13.5 | 102.0 ± 10.2 | 68.8 ± 8.7 | 76.5 ± 8.5 | 119.0 ± 13.5 |
| $L_2$-Cu | 42.7 ± 3.3 | 2.1 ± 0.1 | 50.0 ± 2.4 | 94.9 ± 9.4 | 39.5 ± 2.5 | 116.4 ± 14.6 | 65.3 ± 8.5 | 159.2 ± 19.4 | 95.1 ± 11.1 | 131.7 ± 15.6 |
| $L_3$-Cu | 65.2 ± 2.5 | 63.9 ± 4.3 | 48.3 ± 2.5 | 205.1 ± 20.3 | 362.1 ± 38.1 | 58.3 ± 6.4 | 196.4 ± 22.6 | 134.7 ± 15.6 | 119.5 ± 13.5 | >300 |
| $L_4$-Cu | 58.4 ± 5.8 | 115.8 ± 9.2 | 205.5 ± 25.1 | 198.7 ± 22.5 | 307.5 ± 34.2 | 160.5 ± 18.0 | 296.8 ± 32.4 | 196.8 ± 23.5 | 125.1 ± 14.8 | 105.2 ± 13.5 |
| $L_5$-Cu | 58.8 ± 3.9 | 15.2 ± 1.0 | 26.0 ± 2.5 | 84.4 ± 8.4 | 97.6 ± 9.7 | 32.4 ± 3.2 | 79.2 ± 8.5 | 36.3 ± 3.6 | 46.4 ± 4.6 | 84.3 ± 8.4 |
| $L_1$-Ag | 279.3 ± 12.9 | >300 | 96.8 ± 9.6 | 185.7 ± 16.5 | 207.0 ± 25.6 | 136.7 ± 16.5 | 612.0 ± 61.2 | >300 | 209.7 ± 20.9 | >300 |
| $L_2$-Ag | 31.6 ± 3.2 | 2.8 ± 0.1 | 30.3 ± 3.0 | 24.9 ± 2.5 | 29.1 ± 3.0 | 18.6 ± 1.8 | 28.2 ± 3.5 | 17.8 ± 1.7 | 17.5 ± 17.5 | 22.0 ± 10.2 |
| $L_3$-Ag | 3.3 ± 0.3 | 3.4 ± 0.2 | 9.8 ± 0.9 | 10.1 ± 3.1 | 16.2 ± 1.6 | 4.8 ± 0.4 | 5.1 ± 0.5 | 9.9 ± 0.9 | 9.2 ± 0.9 | 9.5 ± 0.9 |
| $L_4$-Ag | 173.3 ± 10.3 | 139.3 ± 28 | >300 | 240.7 ± 28.5 | 103.6 ± 10.3 | 236.7 ± 28.5 | 136.6 ± 15.8 | 5.5 ± 0.6 | 139.1 ± 16.5 | 284.8 ± 30.5 |
| $L_5$-Ag | 110.7 ± 9.0 | 9.6 ± 0.6 | 148.4 ± 19.5 | 161.6 ± 16.1 | 135.9 ± 13.5 | 100.3 ± 10.1 | 111.7 ± 13.4 | 30.5 ± 4.5 | 110.8 ± 11.0 | 109.4 ± 11.0 |
| 5-FU | 50.2 ± 21.0 | 19.2 ± 1.2 | 22.4 ± 2.5 | 24.2 ± 2.4 | 30.6 ± 3.5 | 37.3 ± 5.8 | 45.5 ± 4.5 | 65.3 ± 8.6 | 142.3 ± 18.6 | 75.3 ± 7.5 |

[a]Values are means of three independent experiments.
[b]$IC_{50}$ values determined at 48 h.

of triazene and phenly rings. The high intensity n→π* band in the range of 341–367 nm occurred due to the conjugation between aromatic ring system and triazene group. The band in the range of 401–531 nm can be regarded as n–π* electronic transition involving the whole electron system with charge transfer interaction within the molecules. The UV absorption band of **$L_5$** in visible region was found to be the highest among all triazene compounds. This is because of the reason that the compound has electron donating groups which causes bathochromic shift to 496 nm. Table 1 shows absorption maxima of all compounds in the visible region and the charge transfer energies ($E_{CT} = 1243{,}667/\lambda_{CT}$) calculated from wavelengths of absorption maxima. When wavelengths of ligands and complexes at visible region were compared, the highest value belonged to **$L_5$** from ligands and **$L_4$-Ag** from complexes. As an electron-transfer trend increases, less energy is required for charge-transfer process and the resulting complex has absorption at greater wavelengths. Wavelengths of silver complexes were higher compared to copper complexes. Low energy bands occurring in 411–461 nm region at electronic spectra of copper (II) complexes and in the range of 423–531 nm in the spectra of silver (I) complex occurred as a result of d-d and metal-to-ligand charge transfers.

$^1$H-NMR and 13C-NMR spectra of all 1,3-diaryltriazene and metal complexes were recorded in DMSO-$d_6$ relative to TMS as reference. Peaks of aromatic hydrogen in the spectra of copper and silver complexes occurred in regions that were similar to their ligands. The most distinct difference in spectra of ligands and complexes was the absence of triazene hydrogen peaks in complex spectra. The – NH – peak was observed around 12.75 ppm in the ligands, but there was no peak around 12.75 ppm in the metal complexes. This was an obvious evidence for that formation of the complex took place through nitrogen atoms of triazene. There is no significant change in peak positions corresponding to the sulfonamide protons in the complexes.

### 3.2. Cytotoxicity studies

In order to investigate the cytotoxic efficiency of novel copper (II) and silver 1,3-diaryltriazene-substituted metanilamide complexes on seven cancer cell lines together with three normal cell lines, MTT assay was performed. The cancer cells included human colorectal adenocarcinoma (DLD-1), cervix carcinoma (HeLa), breast adenocarcinoma (MDA-MB-231), colon adenocarcinoma (HT-29), endometrial adenocarcinoma (ECC-1), prostate cancer (DU-145 and PC-3), and the normal cells used were embryonic kidney (HEK-293), prostate epithelium (PNT-1A), and retinal pigment epithelium (ARPE-19) cells. In the Table 2, $IC_{50}$ values (concentration required to inhibit tumor cell proliferation by 50%) of newly prepared Cu and Ag metal complexes of 1,3-diaryltriazene derivatives were summarised.

In general, from Table 2, it can be seen that Cu (II) and Ag (I) complexes of 1,3-diaryltriazene derivatives showed more cytotoxic efficiency than their ligands. Specifically, the most efficient cytotoxic effect was observed against HeLa cancer cell line with metal complexes of $L_1$-Cu, $L_2$-Cu, $L_2$-Ag, $L_3$-Ag, and $L_5$-Ag with $IC_{50}$ values of 5.02, 2.08, 2.80, 3.40, and 9.61 μM, respectively. Among the series, the metal complex $L_3$-Ag showed greater cytotoxicity against all cancer cell lines with $IC_{50}$ values ranging from 3.30 to 16.18 μM. The compound $L_2$-Ag was also more effective against most of the cancer cell lines as compared to 5-FU with $IC_{50}$ values of 31.56 (DLD-1), 2.80 (HeLa), 29.11 (ECC-1), 18.63 (DU-145) and 28.18 (PC-3) μM. Among the uncomplexed ligands, the most effective cytotoxicity was observed against DU-145 cancer cell line with $IC_{50}$ values in the range of 18.96 to 186.56 μM. More specifically, the ligand $L_1$ showed highest cytotoxicity against prostate cancer (DU-145) ($IC_{50}$: 28.96 M), but, on the other hand, against normal prostate cells (PNT1-A) the cytotoxicity was much lower ($IC_{50}$: 194.89 M) (Figure 1). According to these results, the ligand $L_1$ possessed high selectivity between prostate cancer cell line (DU-145) and normal prostate cells (PNT1-A).

Among the Cu (II) complexes, the $L_2$-Cu showed great cytotoxic activity against all cancer cell lines that were assessed in the this work. Regarding activity against the highest metastised effective HeLa cancer cell line, the $L_2$-Cu emerged as the most active one that displayed cytotoxic activity with $IC_{50}$ value equals to 2.08 μM, which is comparable to the reference drug 5-FU ($IC_{50}$: 19.15 μM) (Figure 2).

On the other hand, investigation of the cytotoxicity towards the cervix carcinoma HeLa cells elucidated that $L_2$-Ag complex had the highest cytotoxicity ($IC_{50}$: 2.80 μM) among the Ag (I) complexes, with 6.84 fold increased potency than the reference drug 5-FU ($IC_{50}$: 19.15 μM) (Figure 3).

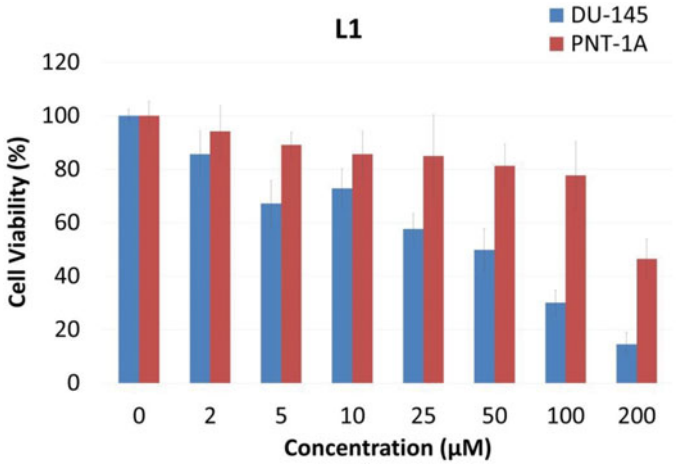


Figure 1. Plot of viable cells at various concentrations of $L_1$ against DU-145 tumor cells and PNT-1A normal cell line.

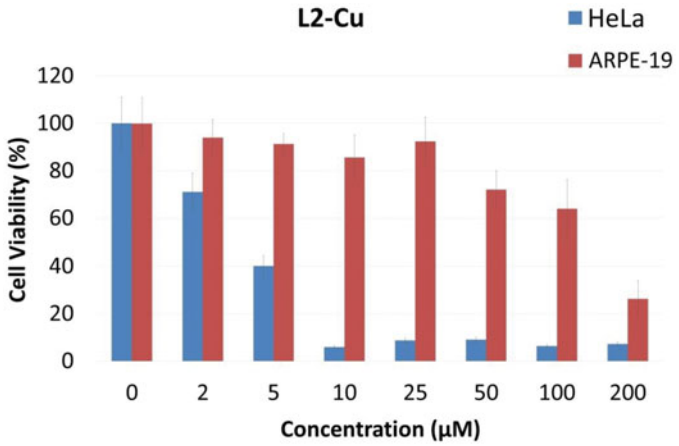


Figure 2. Plot of viable cells at various concentrations of L2-Cu against HeLa tumor cells and ARPE-19 normal cell line.

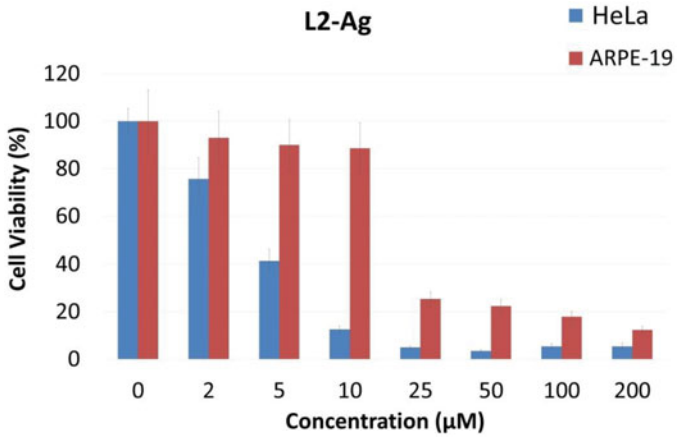


Figure 3. Plot of viable cells at various concentrations of $L_2$-Ag against HeLa tumor cells and ARPE-19 normal cell line.

## 4. Conclusion

We investigated a series of copper (II) and silver (I) complexes of 1,3-diaryltriazene-substituted sulfonamide derivatives. The cytotoxic activity of these ligands and their Cu (II) and Ag (I) complexes were evaluated against seven cancer cell lines (DLD-1, HeLa, MDA-MB-231, HT-29, ECC-1, DU-145, PC-3) as well as three normal cell lines (HEK-293, PNT-1A, and ARPE-19). Most of the metal complexes showed better cytotoxic potency than their ligands and comparable potency to that of 5-Fluorouracil (5-FU), which is a commonly used drug. Specifically, one of the metal complexes (**$L_3$-Ag**) from the series presented great cytotoxic activity against all cancer cell lines that were tested in this study with $IC_{50}$ values in the range of 3.30–16.18 μM. As a result, this work encouraged us to investigate their anticancer profiles in further studies.

## Disclosure statement

No potential conflict of interest was reported by the authors.

## Funding

The authors thank TUBITAK (The Scientific and Technological Research Council of Turkey) for partial financial support [grant no: 216S907].

## ORCID

Claudiu T. Supuran http://orcid.org/0000-0003-4262-0323

## References

1. Hanahan D, Weinberg RA. The hallmarks of cancer. Cell 2000;100:57–70.
2. Harris AL. Hypoxia-a key regulatory factor in tumour growth. Nat Rev Cancer 2002;2:38–47.
3. Semenza GL. Targeting HIF-1 for cancer therapy. Nat Rev Cancer 2003;3:721–32.
4. a) Supuran CT. Advances in structure-based drug discovery of carbonic anhydrase inhibitors. Expert Opin Drug Discov 2017;12:61–88. b) Supuran CT. How many carbonic anhydrase inhibition mechanisms exist? J Enzyme Inhib Med Chem 2016;31:345–60. c) Supuran CT. Carbon-versus sulphur-based zinc binding groups for carbonic anhydrase inhibitors? J Enzym Inhib Med Ch 2018;33:485–95. d) Supuran CT. Structure and function of carbonic anhydrases. Biochem J 2016;473:2023–32.
5. a) Supuran CT, Capasso C. The eta-class carbonic anhydrases as drug targets for antimalarial agents. Expert Opin Ther Targets 2015;19:1:551–63. (b) Akocak S, Ilies MA, Next-generation primary sulfonamide carbonic anhydrase inhibitors. In: Supuran CT, Cappasso C, eds. Targeting carbonic anhydrases, future science. London; 2014:35–51. (c) Vullo D, Del Prete S, Fisher GM, et al. Sulfonamide inhibition studies of theg-class carbonic anhydrase from the malaria pathogen Plasmodium falciparum. Bioorg Med Chem 2015;23:526–31. d) Akocak S, Alam MR, Shabana AM, et al. PEGylated bis-sulfonamide carbonic anhydrase inhibitors can efficiently control the growth of several carbonic anhydrase IX-expressing carcinomas. J Med Chem 2016;59:5077–88. e) Shabana AM, Mondal UK, Alam R, et al. pH-Senstive multiligand gold nanoplatform targeting carbonic anhydrase IX enhances the delivery of doxorubicin to hypoxic tumor spheroids and overcomes the hypoxia-induced chemoresistance. ACS Appl Mater Interf 2018;10:17792–808.
6. a) Supuran CT. Carbonic anhydrases: novel therapeutic applications for inhibitors and activators. Nat Rev Drug Discov

2008;7:168–81. (b) Neri D, Supuran CT. Interfering with pH regulation in tumours as a therapeutic strategy. Nat Rev Drug Discov 2011;10:767–77.
7. a) Akocak S, Lolak N, Nocentini A, et al. Synthesis and biological evaluation of novel aromatic and heterocyclic bis-sulfonamide Schiff bases as carbonic anhydrase I, II, VII and IX inhibitors. Bioorg Med Chem 2017;25:3093–7. (b) Akocak S, Lolak N, Bua S, et al. Synthesis and biological evaluation of novel N,N′-diaryl cyanoguanidines acting as potent and selective carbonic anhydrase II inhibitors. Bioorg Chem 2018; 77:245–51.
8. a) Draghici B, Vullo D, Akocak S, et al. Ethylene bis-imidazoles are highly potent and selective activators for isozymes VA and VII of carbonic anhydrase, with a potential nootropic effect. Chem Commun 2014;50:5980–3. (b) Akocak S, Lolak N, Vullo D, et al. Synthesis and biological evaluation of histamine Schiff bases as carbonic anhydrase I, II, IV, VII, and IX activators. J Enzym Inhib Med Chem 2017;32:1305–12. (c) Senturk M, Gulcin I, Beydemir S, et al. In vitro inhibition of human carbonic anhydrase I and II isozymes with natural phenolic compounds. Chem Biol Drug Des 2011;77:494–9. (d) Carradori S, Secci D, De Monte C, et al. A novel library of saccharin and acesulfame derivatives as potent and selective inhibitors of carbonic anhydrase IX and XII isoforms. Bioorg Med Chem 2016;24:1095–105. (e) Nocentini A, Bua S, Lomelino CL, et al. Discovery of new sulfonamide carbonic anhydrase IX inhibitors incorporating nitrogenous bases. ACS Med Chem Lett 2017;8:1314–19.
9. Pacchiano F, Carta F, McDonald PC, et al. Ureido-substituted benzenesulfonamides potently inhibit carbonic anhydrase IX and show antimetastatic activity in a model of breast cancer metastasis. J Med Chem 2011;54:1896–902.
10. Lou Y, McDonald PC, Oloumi A, et al. Targeting tumor hypoxia: suppression of breast tumor growth and metastasis by novel carbonic anhydrase IX inhibitors. Cancer Res 2011;71: 3364–76.
11. Pacchiano F, Aggarwal M, Avvaru BS, et al. Selective hydrophobic pocket binding observed within the carbonic anhydrase II active site accommodate different 4-substituted-ureido-benzenesulfonamides and correlate to inhibitor potency. Chem Commun 2010;46:8371.
12. a) Kimball DB, Haley MM. Triazenes: a versatile tool in organic synthesis. Angew Chem Int Ed Engl 2002;41: 3338–51. b) Marchesi F, Turriziani M, Tortorelli G, et al. Triazene compounds: mechanism of action and related DNA repair systems. Pharmacol Res 2007;56:275–87.
13. a) Unsalan S, Cikla P, Kucukguzel SG, et al. Synthesis and characterization of triazenes derived from sulfonamides. Marmara Pharm J 2011;15:11–17. b) Zovko TC, Brozovic A, Piantanida I, et al. Synthesis and biological evaluation of 4-nitro-substituted 1,3-diaryltriazenes as a novel class of potent antitumor agents. Eur J Med Chem 2011;46:2971–83. c) Hill DT, Stanley KG, Williams JE, et al. 1,3-Diaryltriazenes: a new class of anorectic agents. J Med Chem 1983;26:865–9.
14. a) Ayala EC, Delgado AV, Moreno GR, et al. Synthesis, structures and catalytic activity of 1,3-bis(aryl)triazenide (p-cymene)ruthenium(II) complexes. Inorganica Chica Acta 2016;446:161–8. (b) MFI V, Llamas SAC, Lucano AAP, et al. Iridium (III) 1,3-bis(aryl)triazenide complexes: synthesis, characterization and structure. Inorganica Chimica Acta 2016; 451:209–15. (c) Vajs J, Steiner I, Brozovic A, et al. The 1,3-diaryltriazenido(p-cymene)ruthenium(II) complexes with a high in vitro anticancer activity. J Inorg Biochem 2015;153:42–8.
15. a) Kia R. A new tetranuclear copper(I) cluster of 1,3-bis(4-bromophenyl)triazene ligand: synthesis, characterization, structural and computational studies. Inorganica Chimica Acta 2016;446:32–40. (b) Rofouei MR, Gharamaleki JA, Melardi MR, et al. Synthesis, characterization and crystal structures of $Hg^{II}$ complexes with asymmetric ortho-functionaized 1,3-bis(aryl)triazenide ligands. Polyhedron 2012;44: 138–42. (c) Rofouei MK, Aghaei A. Synthesis and spectroscopic studies of some new ortho functionalized triazene compounds and their reactivity with mercury (II) ion. J Iran Chem Soc 2013;10:969–77.
16. Frezza M, Hindo S, Chen D, et al. Novel metals and metal complexes as platforms for cancer therapy. Curr Pharm Des 2010;16:1813–25.
17. Bruijnincx P, Sadler P. New trends for metal complexes with anticancer activity. Curr Opin Chem Biol 2008;12:197–206.
18. Mourino V, Cattalini JP, Boccaccini AR. Metallic ions as therapeutic agents in tissue engineering scaffolds: an overview of their biological applications and strategies for new developments. J R Soc Interf 2012;9:401–19.
19. a) Ndagi U, Mhlongo N, Soliman ME. Metal complexes in cancer therapy - an update from drug design perspective. Drug Design Dev Therapy 2017;11:599–616. (b) Apohan E, Yilmaz U, Yilmaz O, et al. Synthesis, cytotoxic and antimicrobial activities of novel cobalt and zinc complexes of benzimidazole derivatives. J Organometallic Chem 2017;828:52–8.
20. a) Lolak N, Akocak S, Bua S, et al. Design and synthesis of novel 1,3-diaryltriazene-substituted sulfonamides as potent and selective carbonic anhydrase II inhibitors. Bioorg Chem 2018;77:542–7. (b) Akocak S, Lolak N, Bua S, Supuran CT. Discovery of novel 1,3-diaryltriazene-substituted metanilamides as carbonic anhydrase I,II,VII and IX inhibitors. J Enzym Inhib Med Chem 2018;33:1575–80. (c) Tuluce Y, Gorgisen G, Gulacar IM, et al. Antiproliferative and apoptotic role of novel synthesized Cu(II) complex with 3-(3-(4-fluorophenyl)Triaz-1-en-1-yl) benzenesulfonamide in common cancer models. Anticancer Res 2018;38:5115–20.
21. a) Koyuncu I, Gonel A, Kocyigit A, et al. Selective inhibition of carbonic anhydrase-IX sulphonamide derivatives induces pH and reactive oxygen species-mediated apoptosis in cervical cancer HeLa cells. J Ezyme Inhib Med Chem 2018;33: 1137–49. (b) Tülüce Y, Ahmed BA, Koyuncu I, Durgun M. The cytotoxic, apoptotic and oxidative effects of carbonic anhydrase IX inhibitor on colorectal cancer cells. J Bioenerg Biomembr 2018;50:107–16.
22. Durgun M, Turkmen H, Zengin G, et al. Synthesis, characterization, in vitro cytotoxicity and antimicrobial investigation and evaluation of physicochemical properties of novel 4-(2-methylacetamide)benzenesulfonamide derivatives. Bioorg Chem 2017;70:163–72.